THE STRUCTURE OF SHOCK WAVES FROM ELECTRODELESS DISCHARGES IN AIR AND ARGON

Z. A. Petchek, R. I. Soloukhin, and S. Zh. Toktomyshev

Zhurnal Prikladnoi Mekhaniki i Tekhnicheskoi Fiziki, Vol. 8, No. 4, pp. 104–110, 1967

Electric discharge shock tubes are now widely used as facilities for the study of physical and chemical processes in shock waves with gas temperatures behind the shock on the order of 10^5° K. The extension of

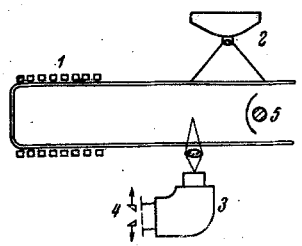

Fig. 1. Schematic of the equipment: 1) discharge coil; 2) camera; 3) spectrograph; 4) photoelectric attachment for recording, as a function of time, the intensities of two emission spectral lines of hydrogen.

the range of gas temperatures and velocities in shock waves produced in this way, in comparison with those from diaphragm shock tubes, stems from the large dynamic range of the expanded magnetic field of the discharge, which is "frozen" in a low density plasma

$$u_{max} \approx H / \sqrt{\pi\rho} \sim 10^7 - 10^9 \text{ cm/sec},$$

while the limiting velocities of unsteady efflux of the "driver" high-enthalpy neutral gases are restricted to values on the order of

$$u_{max} = 2/(\gamma - 1)\, c_0 \approx 8 \cdot 10^5 \text{ cm/sec}.$$

In the practical use of electric discharge shock tubes there are serious difficulties, associated mainly with sharp curtailment, and, as sometimes happens, total absence of the hot "slug" of compressed

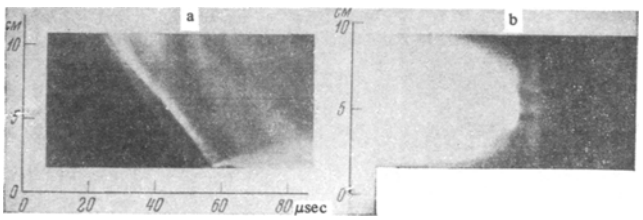

Fig. 2. a) Scan of luminosity from argon, P_1 = 0.7 mm Hg, 27 cm from the coil; b) scan through a transverse slit by the method of compensation of the gas motion.

gas ahead of the gaseous driver piston, i.e., the discharge plasma [1]. Separation of the discharge plasma from the thermal plasma is observed only for initial pressures above 0.05–1 mm Hg, and Mach numbers in air below 30–35, and below 10–15 in argon [2,3]. The use of an electrodeless (inductive) discharge to obtain shock waves, as will be shown below, does not remove this kind of restriction nor does it obviate the difficulty.

The existence of appreciable deviations from uniformity and regularity of the flow in electric shock tubes imposes special requirements for control of the state of the gas behind the generated shock waves, and measurements of the gas temperature distribution are of paramount importance in this regard. In this paper we present results of systematic measurements of plasma temperature distribution behind strong shock waves in air and argon, obtained by three independent methods. A justification is given for the "hydrodynamic" method of measuring temperature in a supersonic plasma stream, as described in [4, 5], based on a comparison with simultaneous spectrographic measurements. A discussion is given of the peculiarities of formation and propagation of shock waves in electrodeless discharge tubes.

1. Description of Equipment and Methods of Measurement. The tests were carried out on the equipment shown schematically in Fig. 1. A 1-μF capacitor, charged to 30 kV, is discharged through an 8-turn coil of length 10 cm, located at the end of a glass tube of diameter 8.6 cm. The period of oscillation of the discharge circuit is 22 μsec, and rupture occurs at pressures of air or argon (usually with addition of 1% hydrogen) in the range $1-10^{-3}$ mm Hg.

Measurement of electron temperature distribution behind the shock wave was performed by the method in which one uses the relative intensities of two spectral lines of hydrogen (Hβ and Hα), the light flux being limited by two slits of width 0.5 mm at the entrance of an ISP-51 spectrograph (chamber with f = 270 mm at a mean dispersion of about 30 Å/mm); separate measurements of the light as a function of time are carried out by means of two photomultipliers. The reduction of the oscillograms, calibration of the channels, and com-

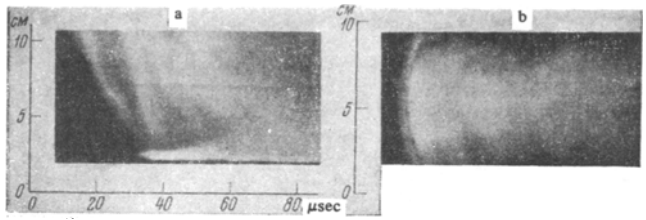

Fig. 3. a) Scan of the process in argon in the discharge and thermal plasma regime, P_1 = 0.05 mm Hg, 27 cm from the coil; b) scan by the method of compensation.

putations of the temperature were analogous to procedures in measurements that we have already published [6]. The estimated error of measurement in this method is 2–3% of the measured quantity.

The other independent method of measuring gas temperature behind the shock was based on measurement of the distribution of the electron concentration in the plasma as a function of time by scanning the luminous spectrum and determining the variation of the half-width of the Hβ hydrogen emission line

$$n_e = 3.4 \cdot 10^{14} \ (\Delta\lambda)^{3/2}.$$

Here the line half-width Δλ is expressed in Å [7, 8]. Scanning of the spectrum was performed with a camera having a linear image speed of 400 m/sec (2.5 μsec/mm). Type RF-3 film was used, and the

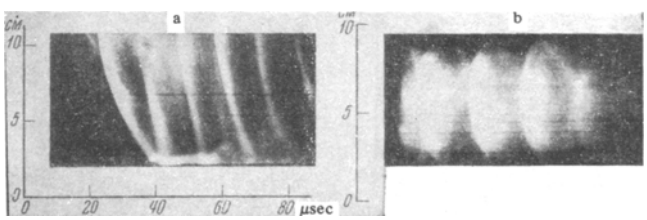

Fig. 4. a) Scan of the process near the coil (7 cm from the end) in argon, P_1 = 0.35 mm Hg; b) scan by the method of compensation.

individual parts of the film were then read on a microphotometer. The error of measurement of electron concentration by this method may be estimated to be on the order of 15–20%, and the appropriate conversion of the data, with the formulas of ionization equilibrium, allows the temperature to be evaluated to an accuracy of about 4–5%,

since

$$\frac{\Delta T}{T} = \frac{2}{5040\varphi / T + 1.5} \frac{\Delta n}{n}.$$

Here φ is the ionization potential of argon, in which the clearest spectral scans were obtained.

Finally, for temperature measurement by the hydrodynamic method, a slit was used to scan the flow of a supersonic stream of plasma behind a shock wave over a model consisting of the lateral surface of a cylinder. The model (diameter = 8 mm, length = 72 mm) was positioned at various distances from the coil, in the central part of the tube cross section. Measurement of the position of the detached shock near the model surface as a function of time allowed determination of the variation of Mach number M of the flow from the well-known dependence of the relative distance on the flow parameter

$$\delta/R = f(M, \gamma).$$

Having the gas velocity from the slope of the traces of the optical disturbances on the same scans, we could determine the velocity of sound from the formula

$$C^2 = [1 + \alpha(\rho, T)]\ \gamma RT/\mu(\rho, T).$$

Here α is the degree of ionization, and μ is the mean molecular weight of the gas. Using tabulated data [9] and calculations [10], it

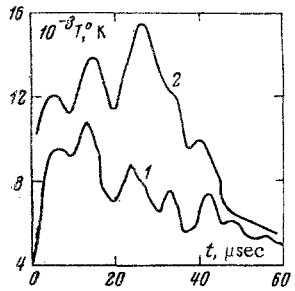

Fig. 5. Variation of temperature behind the shock (argon, p_1 = 0.35 mm Hg, 7 cm from the discharge coil). 1) Oscillogram of luminosity of one of the two measured hydrogen lines (H_β), arbitrary units; 2) profile of temperature variation.

may be established that in the conditions of the above experiments, the speed of sound depends less on density than on temperature: an error in determining the density of the medium even as large as an order of magnitude leads to an error in temperature determination by the above formula of only several percent. Therefore the limit of accuracy of the method is determined mainly by the errors of measurement of the velocity of the medium from the traces of the optical disturbances. Thus, for example, for strongly curved traces, the mean scatter in slope angle measurement in individual parts of the scan can reach 10%, while for relatively constant flow velocity the accuracy of measurement of M may be as low as 1%. The maximum scatter of the temperature data from the hydrodynamic method should nevertheless be estimated as on the order of 15–20%.

In spite of a number of deficiencies (limitation in accuracy, flow disturbance, some inertia because of the time for the shock to be established), the hydrodynamic method of temperature measurement has a number of advantages: a) it is a matter of independent interest in investigation of flow of a plasma over bodies; b) the method is applicable not only in investigations of shock waves, but also in the majority of short-duration facilities such as injectors and plasma accelerators; c) there is interest in using the hydrodynamic method for monitoring during establishment of thermodynamic equilibrium in high-temperature gas streams, along with other methods of diagnosing the state of the gas; and, finally, d) in contrast with the majority of spectroscopic methods, the method allows measurement as a function of time, not of the electron temperature, but of the plasma ion temperature.

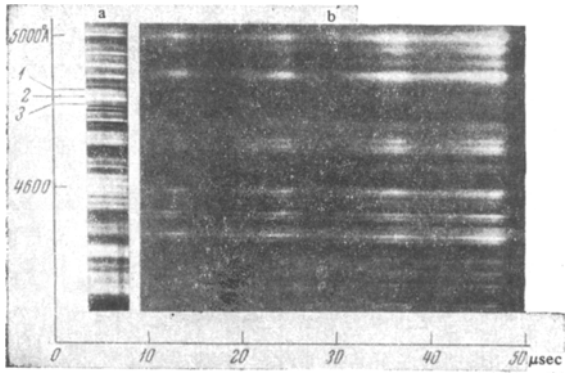

Fig. 6. Luminous spectrum of argon plasma with addition of 1% hydrogen (a) and scan of spectrum 7 cm from coil, p_1 = = 0.35 mm Hg: 1) argon line at 4887 Å; 2) hydrogen line at 4861 Å; 3) argon line at 4847 Å.

2. Description of the Process, and Results of Temperature Measurement. The sequence of hydrodynamic phenomena accompanying electrodeless breakdown of the gas in the tube is illustrated in the photo-scans of plasma self-luminosity (Figs. 2–4), obtained with various arrangements of the camera slit. These show the distribution of luminosity of the gas during stagnation of the flow at the lateral surface of the cylinder mounted in the center of the tube. Because of the difference in brightness, the scans clearly show the distribution of the thermal and the discharge plasma behind a shock wave with relatively low Mach number. The distribution is particularly clear on reflection of the shock from the model surface. Figures 2–4 also give "instantaneous" pictures of the distribution of luminosity at the edge of the expanding plasma "piston," obtained through a slit transverse to the tube axis, in the compensation regime of camera operation, when the image of the object being photographed and the film have no relative motion. On these photographs one may also observe merging of the discharge and thermal plasma, at shock Mach numbers above M_1 = 16 in argon and at pressures below 0.06–0.07 mm Hg. In spite of the fact that mixing of a plasma has already been noted in the literature [1–3], we shall give a discussion below of the causes of this phenomenon.

Figure 5 shows a typical oscillogram of the luminosity of one of the two hydrogen lines in an argon plasma at 7 cm from the end of the coil. The figure also shows the results of reducing the oscillogram data to obtain the distribution of plasma temperature as a function of time at the chosen observation point. It should be noted that similar records, taken at a distance of several tube diameters from the coil, exhibit a smoother variation of luminosity, as may also be seen on the scans of Figs. 2 and 3. The distribution of luminosity in air, apart from the difference in signal amplitude, differs little from that obtained in argon.

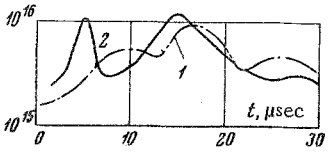

Fig. 7. Profile of variation of electron concentration behind the shock in argon, from a scan of the spectrum at a distance of 7 cm from the coil. 1) p_1 = = 0.1 mm Hg; 2) p_1 = 0.35 mm Hg.

The luminous spectrum of an argon plasma with addition of 1% hydrogen, and scans of the spectrum taken in the central part of the

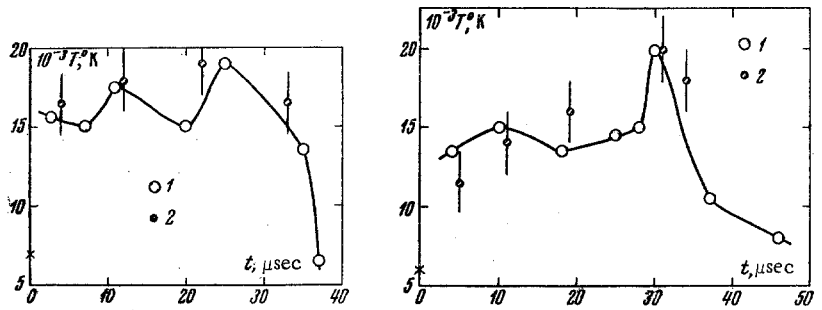

Fig. 8. Comparison of the data on variation of temperature behind the shock in air, 7 cm from the end of the coil. 1) spectral measurements; 2) hydrodynamic method: a) p_1 = 0.35 mm Hg; b) p_1 = 0.7 mm Hg. The cross on the y-axis indicates the calculated value of equilibrium thermal plasma temperature for the given shock velocity.

tube located 7 cm from the end of the coil, are shown in Fig. 6. It can be seen that the luminosity of the argon and hydrogen lines begins practically simultaneously. Figure 7 gives data on the distribution of electron concentration as a function of time, as obtained from scans of the spectrum, as per the variation of the half-width of the H_β line for two different experiments conducted at various initial gas pressures. The data on temperature distribution, as determined from the electron concentration found in this way for argon, will be compared later with results of temperature measurement by other methods.

Figure 8 compares the measured variation of temperature behind the shock in air for two different tests carried out at a distance of 7 cm from the end of the coil. The cross on the y-axis indicates the calculated value of equilibrium thermal air plasma temperature behind a shock with the appropriate speed. The graphs show that the spectroscopic data and the temperature measurements by the hydrodynamic method agree within the limits of the experimental accuracy. The smoother variation of the "hydrodynamic" data is due, as has already been noted, to the inertia represented by the finite time for the shock to form at the body surface. It may also be seen that near the coil the measured temperature is appreciably higher than the calculated "gasdynamic" value. The reason is that in this case (near the coil) it is the temperature of the discharge plasma that is measured, since no separation of the discharge plasma from the thermal plasma can be seen on the photo-scans for this condition.

Similar measurements for argon are compared in Fig. 9 with data on the temperature distribution obtained from measurements of the variation in electron concentration. Here too there is good agreement between the results from the three independent methods of temperature measurement. Finally, Fig. 10 shows measurements for two different regimes of shock-wave propagation in argon, far (27 cm) from the end of the coil. Despite the difference in the shape of the temperature profile behind the shock, the hydrodynamic and the spectroscopic methods here give results which agree closely. It should be noted that the fluctuations in gas velocity behind the shock diminish rapidly with increasing distance from the "shock" coil, in fact from ±25% at L = 7 cm to ±10% at L = 27 cm. Similar determinations of the variation of flow Mach number are ±10 and ±3%, at a mean Mach number of 1.7–2.0. The effect of separation of the discharge and thermal plasmas is more conspicuous at relatively great distance from the coil (see, for example, Fig. 10a).

3. Discussion of the Results, and Conclusions. It follows from the data obtained under the conditions of the tests described, both in the discharge plasma and in the thermal "slug" (where it exists), no deviations from thermodynamic equilibrium were observed. This is clearly evident from the agreement of the measurement results for the temperature of the medium by the three independent methods, which differ in principle. It is important to note that for relatively large shock Mach numbers, when the thermal and discharge plasmas have already separated, the measured temperature of the gas which has expanded for less than 5 μsec is in good agreement with equilibrium calculations obtained for one-dimensional shock waves in argon. To illustrate this agreement, Fig. 11 shows the ratio of the measured temperature near the shock to the calculated value, for various initial pressures in argon. The same graph gives values of Mach number of the shock in tests chosen for reduction. We note that the Mach number of the shocks generated in an electrodeless discharge depends only slightly on the initial gas pressure, in the range of variation 0.01–0.7 mm Hg.

As regards practical application of electrodeless shock tubes, an important matter is the estimation of "practical" conditions for generating shock waves with separation of the thermal and discharge plasmas. We shall try, in the following way, to evaluate limiting shock wave Mach numbers above which jets of discharge plasma must penetrate into the thermal slug in the central region of the tube cross section. By taking account of the existence of appreciable magnetic pressures in the discharge plasma, we can predict basic variations in the hydrodynamic conditions when it flows into a medium with a finite pressure, when the characteristic thickness of the skin layer in the thermal slug being formed is comparable with the tube radius. The central and the wall region of the flow will not be equivalent in this case from the viewpoint of hydrodynamic resistance to flow of the discharge plasma, since the field, and therefore the resistance, in the central part of the tube, must be less than at the periphery. For lower Mach numbers, i.e., for less conductivity of the thermal plasma and larger skin thickness, the magnetic field will penetrate freely into

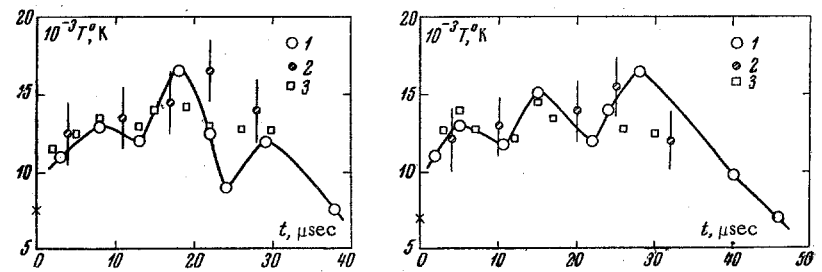

Fig. 9. Comparison of data on temperature behind the shock in argon, 7 cm from the coil. 1) spectral measurements; 2) hydrodynamic method; 3) determination of temperature from data on electron concentration; a) p_1 = 0.1 mm Hg; b) p_1 = 0.35 mm Hg.

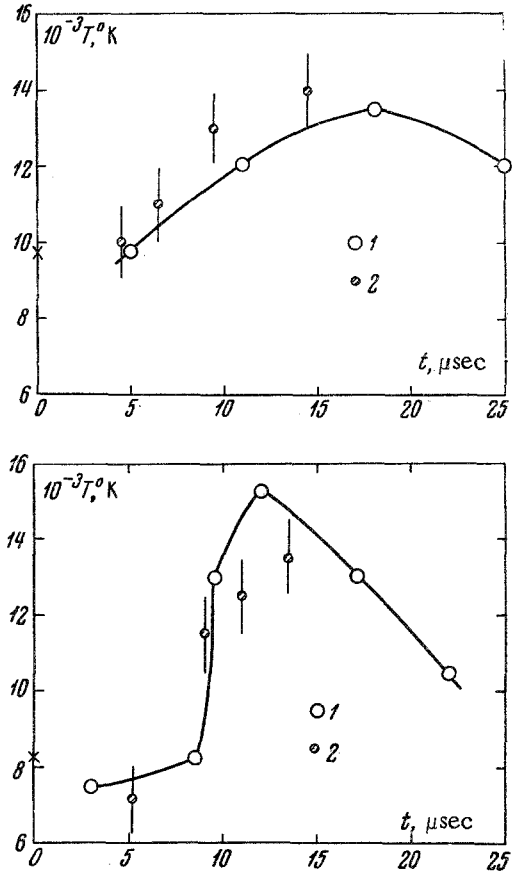

Fig. 10. Comparison of the data on variation of temperature behind a shock in argon, 27 cm from the coil. 1) spectral measurements; 2) hydrodynamic method; a) p_1 = 0.6 mm Hg, b) p_1 = 0.08 mm Hg.

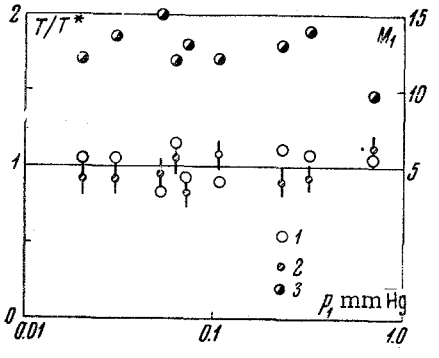

Fig. 11. Comparison of data on temperature, as measured by the various methods, near the shock with the calculated equilibrium temperature T* of a thermal argon plasma behind a one-dimensional shock wave. 1) Spectral measurements; 2) hydrodynamic method. The measurements were made under conditions where the discharge and thermal plasmas are "separated." The values of Mach number of the shocks for each test are also shown (3).

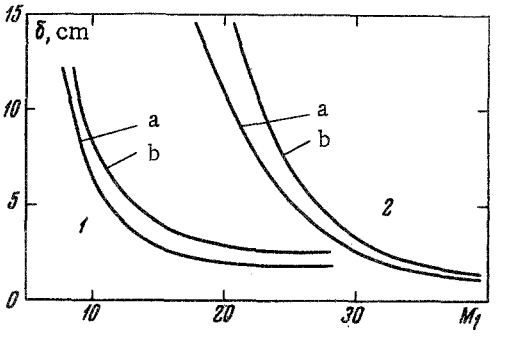

Fig. 12. Results of calculation of characteristic length of the skin-layer in a thermal plasma behind the shock waves in argon (1) and air (2). a) Tube radius R = 2 cm, b) R = 4 cm.

the thermal plasma, and the flow must be roughly the same as in diaphragm shock tubes.

For convenience in estimates of this kind, Fig. 12 shows calculated graphs of the variation of skin thickness in the gas behind the shock in air and argon, as calculated from the formula

$$\delta^2 = c^2R/4\pi\sigma u ,$$

where σ is the conductivity and u is the velocity of the gas for various values of tube radius R as a function of Mach number at an initial gas pressure of 1 mm Hg. By comparing the data of various authors [2, 3, 5, and 11], obtained in electric discharge tubes of various configurations, it can be verified that the above method of evaluating "critical" Mach numbers ($M = M_*$) of the shock waves is in full agreement with the values $M = M_0$ from experimental observations; the formation of the slug is curtailed at just those flow conditions under which the thermal plasma becomes a good conductor. The results of this comparison are given below, indicating the tube radii (R, in mm), the initial pressure (ρ_0, in mm Hg), and the references; the data of the present paper are on the first line.

	R	ρ_0	M_*	M_0	
Argon	40	0.01—0.7	16	16—17	
Argon	5—15	1—10	17	16—19	[3]
Air	15	0.2—0.5	35	35—37	[2, 5]
Air	28.5	0.5—0.7	32	25—40	[11]

In conclusion, the authors wish to express their appreciation to V. Kikhtenko and A. Kocheev for assistance in conducting the experiments.

REFERENCES

1. M. Cloupeau, "Interpretation of luminous phenomena observed in electromagnetic shock tubes," Phys. Fluids, 6, 679, 1963.

2. R. I. Soloukhin, "The stream structure and bow waves in electromagnetic shock tubes," Proc. VII Intern. Confer. on Phenomena in Ionized Gases, Belgrad, p. 800, 1966.

3. A. Hermel and K. Seliger, "Untersuchungen über das Auftreten selbstleuchtender Stossfronten in elektromagnetisch betriebenen Stobrohren," Monatsber Dtsch. Akad. der Wissensch. aften zu Berlin, 4, 7, 287, 1965.

4. Z. A. Pietrzyk, "Speed measurement of gas and sound downstream of a shock wave in an electromagnetic shock tube," Archiwum mechaniki stosowanei, 2, 16, 1964.

5. M. I. Vorotnikova and R. I. Soloukhin, "Flow structure in electric shock tubes," PMTF, no. 5, p. 138, 1964.

6. R. I. Soloukhin and S. Zh. Toktomyshev, "Measurement of temperature behind a detonation front in a gas," PMTF [Journal of Applied Mechanics and Technical Physics], no. 5, p. 124, 1965.

7. P. D. Dikerman, "Spectroscopic determination of plasma temperature," collection: Production and Investigation of High Temperature Plasmas [Russian translation], Izd. Inostr. lit., p. 178, 1962.

8. A. P. Dronov, A. G. Sviridov, and N. N. Sobolev, "Investigation of the state of krypton behind a shock wave," Optika i spektroskopiya, vol. 10, no. 3, p. 312, 1961.

9. N. M. Kuznetsov, Thermodynamic Functions and Shock Adiabats for Air at High Temperature [in Russian], Izd. Mashinostroenie, 1965.

10. N. R. Jones and M. McChesney, "Equilibrium ionization calculations for normal and oblique shock waves in argon," Proc. Phys. Society, vol. 181, 2, p. 223, 1963.

11. Yu. V. Makarov and A. M. Maksimov, "Investigation of the structure of a luminous front in electromagnetic tubes," ZhTF, vol. 35, 2, p. 223, 1965.

18 March 1967 Warsaw, Novosibirsk